



ARTICLE

Fabrication of UV-Curing Linalool–Polysiloxane Hybrid Films with High Refractive Index and Transparency

Wenqing Xiao^{1,#}, Lewen Tan^{1,2,#}, Xunjun Chen^{1,*}, Qiaoguang Li^{1,*} and Yunqing Ruan¹

¹College of Chemistry and Chemical Engineering, Zhongkai University of Agriculture and Engineering, Guangzhou, 510225, China

²R&D Department, Guangzhou Silicon Core Material Technology Co., Ltd., Guangzhou, 510220, China

*Corresponding Authors: Xunjun Chen. Email: cxj.qiao@163.com; Qiaoguang Li. Email: liqiaoguang8799@163.com

#Wenqing Xiao and Lewen Tan contributed equally to this work

Received: 10 October 2023 Accepted: 20 December 2023 Published: 11 April 2024

ABSTRACT

In this article, a series of high refractive indices (1.50–1.53) thiol phenyl polysiloxane (TPS) were synthesized via hydrolytic sol–gel reaction. The Fourier transform infrared spectra (FT–IR) and nuclear magnetic resonance spectra (NMR) results showed that TPS conformed to the predicted structures. Natural terpene linalool was exploited as photocrosslinker to fabricate UV–curing linalool–polysiloxane hybrid films (LPH) with TPS via photoinitiated thiol–ene reaction. LPH rapidly cured under UV irradiation at the intensity of 80 mW/cm² in 30 s, exhibiting good UV–curing properties. The optical transmittance of LPH in the wavelength of 300–800 nm was over 90%, exhibiting good optical transparency. The water contact angle and water vapor permeability results showed that the introduction of phenyl groups enhance the hydrophobicity and water vapor barrier properties of LPH. The results indicated the potential of LPHs in the applications of optical functional coatings.

KEYWORDS

UV–curing; polysiloxane hybrid films; high refractive index; transparency

Nomenclature

TPS	Thiol phenyl polysiloxane
LPH	Linalool–polysiloxane hybrid films
MPTMS	3–mercaptopropyltrimethoxysilane
PTMS	Phenyltrimethoxysilane
MM	Hexamethyldisiloxane
PETA	Pentaerythritol triacrylate
TFA	Trifluoromethanesulfonic acid
FTIR	Fourier transform infrared spectroscopy
NMR	Nuclear magnetic resonance spectroscopy
TMS	Tetramethylsilane
TGA	Thermogravimetric analysis
DSC	Differential scanning calorimetry
RI	Refractive indices



This work is licensed under a Creative Commons Attribution 4.0 International License, which permits unrestricted use, distribution, and reproduction in any medium, provided the original work is properly cited.

YI	Yellow index
WCA	Water contact angle

1 Introduction

Phenyl groups in the main chain and in the pendant chain of polysiloxane endow various special properties, such as thermal stability and water vapor barrier property [1]. Besides, phenyl groups with high molar refraction enhance the refractive index of polysiloxane. High refractive index phenylpolysiloxane resin have been applied in the fields of optoelectronics like optical encapsulant and waveguide materials [2]. High refractive index polysiloxane resin is mainly fabricated by thermal-induced hydrosilylation [3–6]. Whereas traditional thermal curing has shortcomings, such as low reaction rate, high curing temperature and chain transfer side reactions, ultraviolet light curing (UV-curing) with advantages of low energy cost, high reaction rate and wide adaptability over thermal polymerization [7], have widely applied on coatings [8–11], 3D printing materials [12–15], light emitting diode (LED) encapsulant [16,17] and self-healing materials [18,19].

UV-curing is an efficient method to fabricate high refractive index and optical transparent crosslinked polysiloxanes. UV-curing systems are mainly divided into two parts, free radicals polymerization [20,21] and cationic polymerization [22,23]. To obtain UV-curable transparent polysiloxanes, photosensitive functional groups such as (meth)acryloyloxy groups, thiol-ene groups, or epoxy groups should be introduced [24–27]. Presently, lots of researches and industrial applications are based on free radical induced (meth)acrylates polymerization. Gan et al. fabricated a silicone resin with a ladder-like polysilsesquioxane containing acrylic and phenethyl sulfide groups with styrene-modified mercaptopropyl-polysilsesquioxane [16]. The silicone resin UV-cured in 2 min which was transparent and possessed a high refractive index of 1.545 (@450 nm). Compared to the commercial encapsulant, the self-keeping hemisphere-shaped resin enhanced GaN blue LED a light extraction efficiency of 25.6%. However, free radicals polymerization has problems of oxygen inhibition and volume shrinkage [28–30]. Especially, oxygen inhibition affects polymerization mostly. Radicals in photoinitiators and oligomers would be quenched by oxygen in the ambient environment that leading the polymerization termination. Thiol-ene click reaction is one of the photoinitiated polymerizations, which has a high reaction rate and adapts to various olefins. Furthermore, thiol-ene click reaction is insensitive to oxygen which is a facile and efficient method to prepare photocrosslinked networks [31,32]. Sulfur atoms with high molar refraction enhance matrix polymers refractive index so that thiol-ene click reaction is usually used for fabricating high refractive index UV-curing materials [33]. Kim et al. synthesized mercaptopropyl-phenyl-oligosiloxane with diphenyldisilanol and 3-mercaptopropyltrimethoxysilane via sol-gel method and obtained phenyl-sulfur hybriimer with a refractive index of 1.5847 via photoinitiated thiol-ene reaction [34].

Bio-based material is a sustainable resources to prepare composite materials [35,36]. Linalool is a naturally obtained and low-priced terpene alcohol. Based on its pleasant scent and anti-bacterial properties, linalool is now widely used as a perfume and anti-bacterial agents [37]. A linalool molecule contains two unsaturated double bonds that can be used as reaction sites to and introduced to UV-curing system via thiol-ene reaction [38]. Herein, we control the molar ratio of silane monomers to synthesize various photosensitive thiol phenyl polysiloxane (TPS) with different molecular weight hydrolytic sol-gel reactions. And we prepared optical transparent UV-curing linalool-polysiloxane hybrid films (LPH) with TPS and natural terpene linalool via photo activated thiol-ene reaction. The structures and UV-curing properties of LPH were characterized, and so were the effect of phenyl content on the properties of LPH investigated.

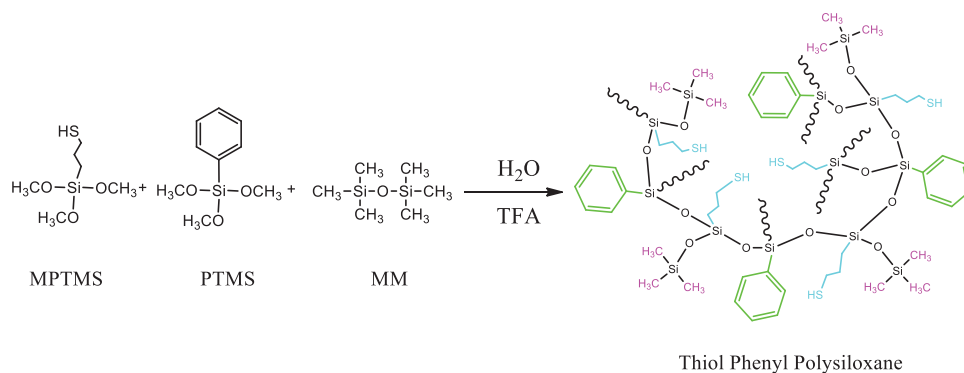
2 Materials and Methods

2.1 Materials

3-mercaptopropyltrimethoxysilane (MPTMS), Phenyltrimethoxysilane (PTMS), Hexamethyldisiloxane (MM) were obtained from Guangzhou Suntop Fine Chemical Co., Ltd., Guangzhou, China. Linalool and Pentaerythritol triacrylate (PETA) were purchased from Shanghai Macklin Biochemical Co., Ltd. Trifluoromethanesulfonic acid (TFA) that used as catalyst was also purchased from Shanghai Macklin Biochemical Co., Ltd., Shanghai, China. 1-Hydroxycyclohexyl phenyl ketone (photoinitiator IRGACURE[®]184) that used as photoinitiator was obtained from Jiangmen Jiuguansong Polymer Materials Co., Ltd., Jiangmen, China. All the reagents were used as received. Deionized water was used throughout the experiment. All chemicals were used as received.

2.2 Synthesis of High Refractive Index Thiol Phenyl Polysiloxane (TPS)

MPTMS, PTMS, MM, and TFA were added into a four-necked round bottom flask equipped with a thermometer, reflux condenser, and magnetic stirrer. The contents of the flask were heated to 40°C and deionized water was added dropwise to the flask over 30 min using a syringe pump. The reaction was allowed to proceed under reflux at 65°C over 3 h. The water and side product methanol were removed by distillation at a nitrogen atmosphere until the temperature of the reactant in the flask reached 95°C. The polymerization reaction allowed to continue in refluxing toluene with the removal of water over 2–3 h until no water remained. Excess Na₂CO₃ was added to neutralize the acid catalyst. The product solution was washed by water several times to remove sodium trifluoromethanesulfonate thoroughly. The clear solution was obtained after adding active carbon and being filtered multiple times. The transparent viscous product was obtained after vacuum distillation to remove the solvent at 150°C. Scheme 1 shows the scheme of synthesis of thiol phenyl polysiloxane. Table 1 shows the specific compositions for each sample and theoretical phenyl content and thiol content.



Scheme 1: Synthesis of thiol phenyl polysiloxane

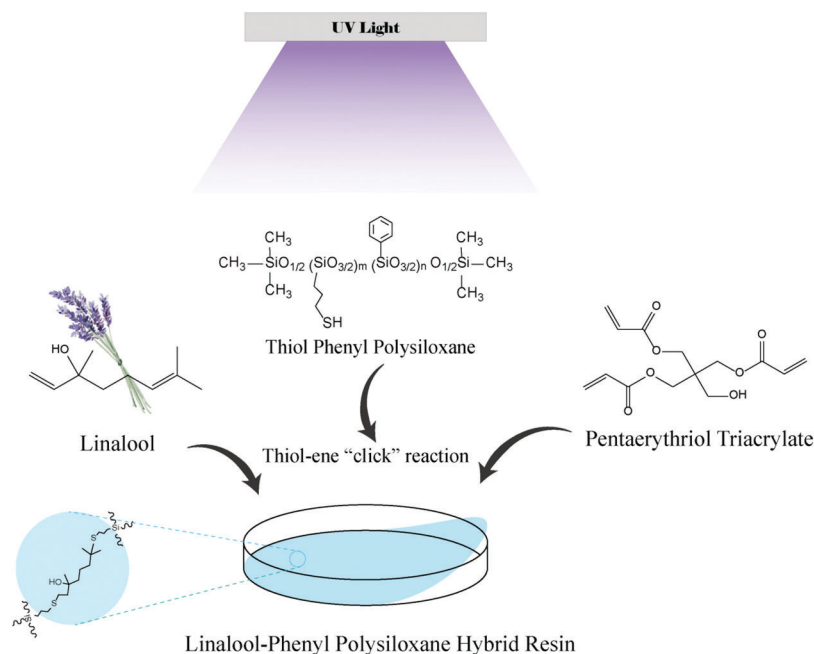
Table 1: Specific compositions of thiol phenyl polysiloxanes

Sample No.	Amount of silane monomers (mmol)			Phenyl content ^a (mmol/g)	Thiol content ^a (mmol/g)
	MPTMS	PTMS	MM		
TPS01	50	50	10	3.46	3.46
TPS02	50	50	20	3.11	3.11
TPS03	50	50	30	2.82	2.82
TPS04	50	50	40	2.59	2.59
TPS05	50	50	50	2.39	2.39

Note: a Calculated values.

2.3 Fabrication of UV-Curing Linalool-Phenyl Polysiloxane Hybrid Film (LPH)

The fabrication of UV-curing linalool-phenyl polysiloxane hybrid film is shown in Scheme 2. The molar ratio of thiol groups and linalool double bonds was set to 1:1. A certain amount of TPS, linalool, 25 wt% PETA, and 5 wt% photoinitiator 184 was mixed uniformly and removed bubbles under a vacuum condition. Transparent films were cast on glass slides using a 200 μm applicator and were UV irradiated at 365 nm with an intensity of 80 mW/cm^2 for 30 s at room temperature (see Scheme 2).



Scheme 2: Fabrication of UV-curing linalool-phenyl polysiloxane hybrid film

2.4 Characterization and Measurements

2.4.1 FTIR Spectroscopy

Fourier transform infrared (FT-IR) spectra were measured using Perkin Elmer FT-IR spectrum 100 at room temperature. The samples were cast on KBr pellets and scanned within the range from 450 to 4000 cm^{-1} over eight times.

2.4.2 NMR Spectroscopy

Proton nuclear magnetic resonance ($^1\text{H-NMR}$) and silicon nuclear magnetic resonance ($^{29}\text{Si-NMR}$) spectra were recorded using a Bruker AVANCE AV 400 MHz spectrometer at room temperature. CDCl_3 was used as the solvent and tetramethylsilane (TMS) was used as an internal reference.

2.4.3 Gel Permeation Chromatography

The weight average molecular weight (M_w) and polydispersity index (PDI, M_w/M_n) of were measured using Agilent 1260 Infinity II GPC/SEC system equipped with a refractive index detector and tetrahydrofuran was used as an eluent at a flow rate of 1 $\text{mL}\cdot\text{min}^{-1}$.

2.4.4 DSC

Glass transition temperature (T_g) was measured using TA Q2000 differential scanning calorimetry in a nitrogen atmosphere. The temperature was increased from -70°C to 100°C at a heating rate of $10^\circ\text{C}\cdot\text{min}^{-1}$.

2.4.5 Thermal Gravimetric Analysis (TGA)

TGA was carried out at a Mettler–Toledo TGA2 thermo gravimetric analyzer in a nitrogen atmosphere (at a flow rate of 20 mL/min) from 40°C to 700°C at a heating rate of 10°C·min⁻¹.

2.4.6 Refractive Indices

Refractive Indices were measured using a Shanghai Optical Instrument Factory WZS–1 Abbe refractometer at 25°C.

2.4.7 Transmittance

The optical transmittance was measured using Shimadzu UV–1800 UV–Vis spectrophotometer in the 200–800 nm wavelength range. Yellow index (YI) was calculated by the following Eq. (1):

$$YI = \frac{T_{680\text{nm}} - T_{420\text{nm}}}{T_{560\text{nm}}} \quad (1)$$

2.4.8 Water Contact Angle

Water contact angle (WCA) was measured using a Biolin Theta automatic contact angle meter. The measurements were carried out in triplicate and average values were calculated.

2.4.9 Moisture Barrier Property

The moisture barrier property was measured using a Labthink W3/030 water vapor transmittance tester at 38°C with a gradient of 90%–0% relative humidity across the film.

2.4.10 The UV–Curing Behavior

The UV–curing behavior was investigated by monitoring the degrees of thiol groups and ene groups conversions with a Perkin Elmer Spectrum 100. The samples were cast on KBr pellets and UV–irradiated at the intensity of 80 mW/cm². The spectra under various irradiation times were recorded.

$$C\%_{\text{SH}} = \frac{(A_{2571}/A_{1735})_{t_0} - (A_{2571}/A_{1735})_{t_1}}{(A_{2571}/A_{1735})_{t_0}} \quad (2)$$

$$C\%_{\text{C=C}} = \frac{(A_{1638}/A_{1735})_{t_0} - (A_{1638}/A_{1735})_{t_1}}{(A_{1638}/A_{1735})_{t_0}} \quad (3)$$

The degrees of thiol groups and ene groups conversions were calculated by Eqs. (2) and (3), respectively. A_{2571} and A_{1638} represented the peak area of thiol groups and ene groups. A_{1735} represented the peak area of carbonyl group which acted as a reference group.

3 Results

3.1 Synthesis and Characterization Of Thiol Phenyl Polysiloxane

In this work, 3–mercaptopropyltrimethoxysilane (MPTMS), phenyltrimethoxysilane (PTMS), hexamethyldisiloxane (MM) were used as reactive monomers to synthesize UV–curable high refractive index thiol phenyl polysiloxane (TPS) via hydrolytic sol–gel reaction under acid condition. As shown in Table 1, the molar ratio of MM was precisely controlled to obtain TPS with various molecular weights and refractive indices. As shown in Fig. 1, FT–IR analysis was further carried out to characterize the molecular structure of TPS. The peak at 2840 cm⁻¹ was not detected which indicated the methoxyl groups on silicon atom hydrolyzed into silanol groups entirely. Meanwhile, a wide asymmetric peaks around 1137 and 1056 cm⁻¹ appeared which could be attributed to the asymmetric Si–O–Si stretching on polysiloxane T units ((RSiO_{1.5})_x), indicating the condensation between silanol groups and the formation of stable polysiloxane structure under catalytic effect of TFA. The broad peaks at 3648 cm⁻¹ could be ascribed to the uncondensed silanols which were caused by the steric hindrance effect of phenyl groups. The peak at 2571 cm⁻¹ originated from the thiol group, indicating that the thiol moiety retained after the hydrolytic sol–gel reaction and be available for the photo crosslinking. A sharp peak at 1255 cm⁻¹

resulted from methyl groups connecting on silicon atoms. The peaks at 1431 cm^{-1} resulted from the bending vibration of the C–H bond and the peaks at 2958 cm^{-1} resulted from the asymmetric stretching vibration of C–H bond. The peaks at 1595 cm^{-1} resulted from the backbone vibration of C=C bond on phenyl group. In summary, the predicted structure of TPS was characterized preliminary by FT–IR.

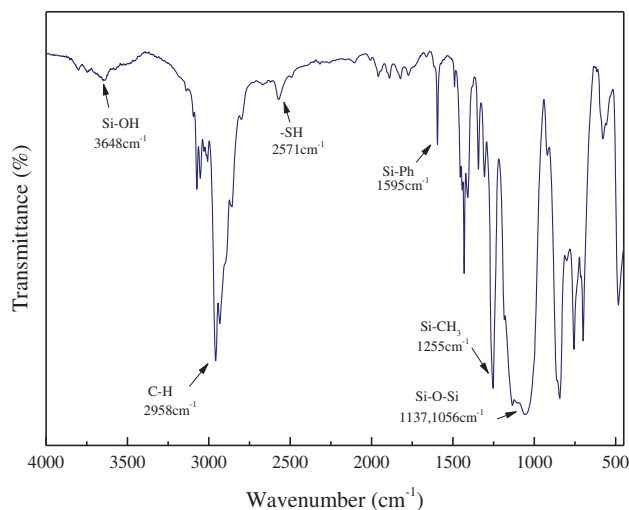


Figure 1: FT–IR spectrum of thiol phenyl polysiloxane

In order to confirm the molecular structure of TPS, ^1H -NMR and ^{29}Si -NMR were carried out as well. The ^1H -NMR spectrum of TPS02 is shown in Fig. 2. The peaks at 7.64–7.39 ppm (Si–C₆H₅) were assigned to the phenyl protons. And the mercaptopropyl propylene protons located at 2.55–2.26 ppm (Si–CH₂CH₂CH₂SH), 1.73–1.57 ppm (Si–CH₂CH₂CH₂SH) and 0.83 ppm (Si–CH₂CH₂CH₂SH), respectively. The thiol proton is located at 1.35–1.25 ppm. Compared with the TMS signal at 0 ppm, a sharp peak at 0.12 ppm was assigned to methyl proton in TPS. A slight field shift demonstrated that MM incorporated to the polysiloxane structure. The methoxyl proton signal was not detected at 3.5–3.6 ppm, indicating that oxygen atoms on methoxy groups protonated and hydrolyzed into silanol entirely under acid conditions [39].

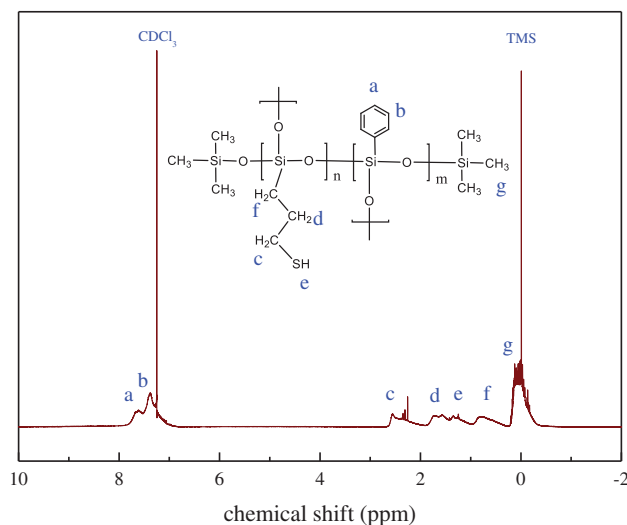


Figure 2: ^1H -NMR spectrum of thiol phenyl polysiloxane

As we can see, the ^{29}Si -NMR spectrum of TPS02 shown in Fig. 3 was divided into two parts. The signal at 11.06 ppm is attributed to the M unit ($(\text{CH}_3)_3\text{SiO}_{1/2}$) on TPS. The low field signals at 66.78 and 78.70 ppm resulted in the T^3 units ($(\text{HSCH}_2\text{CH}_2\text{CH}_2\text{SiO}_{3/2})$ and $(\text{Ph-SiO}_{3/2})$) condensed from MPTMS and PTMS, respectively, demonstrating spatial networks and capping structures formed in TPS. Few weak signals at 54.04 and 69.91 ppm were detected as well which originated from the T^2 units, demonstrating the silanol condensed incompletely due to the steric hindrance effect [34,40]. The structure of TPS was characterized by NMR and FT-IR spectra and the results coincided with expectation, confirming that TPS was successfully synthesized via hydrolytic sol-gel reaction.

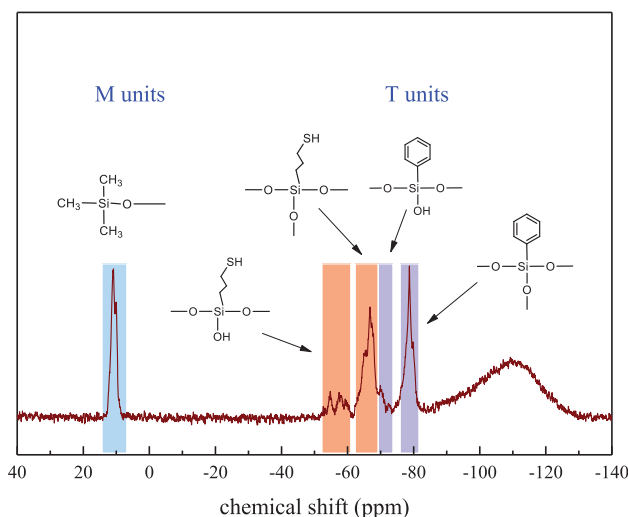


Figure 3: ^{29}Si -NMR spectrum of thiol phenyl polysiloxane

Thermal stability is one of the most important properties of polymer materials. The thermal decomposition spectra of TPS from 40°C to 700°C are shown in Fig. 4 and Table 2. The mass residual ratio (R_w) of TPS increased from 11.64% to 64.35% and the temperature at 5% mass loss ($T_{5\%}$) increased from 191.83°C to 318.50°C. With the reduction of monofunctional end-capping segment, TPS inclined to form a more condensed and stable three-dimension crosslinking polysiloxane structure, resulting in thermal stability enhanced remarkably. Besides, the pendent aromatic rings were capable of alleviating the unbuttoned and thermal degradation of siloxane chains under high temperatures.

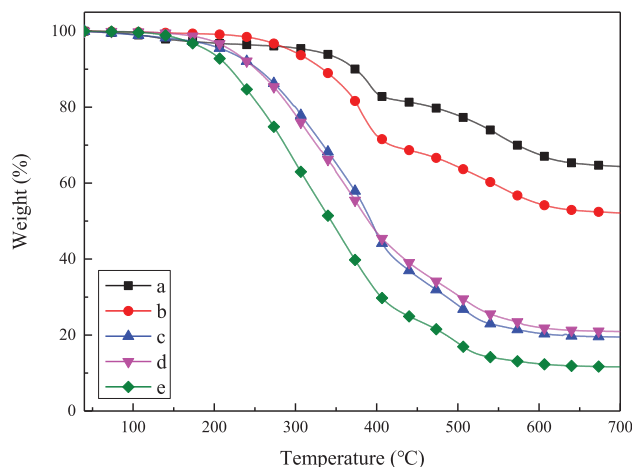


Figure 4: TGA curves of samples TPS. (a)TPS01, (b) TPS02, (c) TPS03, (d) TPS04 and (e) TPS05

Table 2: Synthetic results, optical and thermal properties of TPS

Sample No.	M _w (kDa)	PDI	Glass transition temperature (T _g /°C)	Refractive index (n _D ²⁵)	T _{5%} (°C)	T _{10%} (°C)	R _w (%)
TPS01	6.83	3.30	-4.95	1.5361	318.50	373.50	64.35
TPS02	3.82	2.44	-29.55	1.5200	294.17	333.83	52.15
TPS03	2.28	2.28	-56.19	1.5055	213.33	254.17	19.50
TPS04	1.91	1.85	-61.63	1.4962	221.17	251.67	20.91
TPS05	1.54	1.68	-67.60	1.4875	191.83	220.00	11.64

As outlined in Table 2, GPC results showed that the weight average molecular weight increased from 1.54 to 6.83 kDa. M_w of TPS increased with the decline of MM ratio, illustrating MM hydrolyzed and form end-capping structure to terminate the growing polymer chains under acid conditions. In addition, the polydispersity indices (PDI) were at low values, indicating that MM regulated the condensation of silane monomers and synthesized polymers with concentrated molecular weights. However, with less introduction of MM, polysiloxanes with more random structures formed resulting in molecular weight distribution became wide. DSC results indicated glass transition temperature rose with higher molecular weight. Besides, TPS with higher molecular weights contained a more rigid benzene structure and the π - π stacking interaction between aromatic rings caused the decline of polymer chain flexibility [41].

The appearance of synthesized TPS was transparent viscous liquid and the refractive indices ranged from 1.48 to 1.53. According to the Lorentz-Lorenz equation, introducing aromatic rings and sulfur atom with high molar refractions to the polymer chains endowed high refractive indices of TPS [42]. TPS exhibited decent optical properties which showed its potential applications as optical materials, such as LED encapsulants and optical device coatings.

3.2 Thermal Stabilities of UV-Cured LPH

Linalool is a natural terpene alcohol with a pleasant scent and antibacterial properties which was applied in perfumed products and antibacterial agents. But there are few researches and applications of linalool in the fields of functional materials. Therefore, we utilized two unsaturated double bonds in linalool to synthesize UV-curable bio-based hybrid polysiloxane optical films with TPS via thiol-ene click reaction.

The thermal properties of all LPH samples were studied and the results are shown in Fig. 5 and Table 3. Compared with TPS prepolymers, the R_w of LPH03, LPH04 and LPH05 enhanced obviously which was caused by the photocrosslinking between thiol and ene groups in TPS and linalool, leading to the thermal stability improved. Contrarily, the thermal stability of LPH01 and LPH02 was slightly reduced because polymer chain segments containing benzene rings were difficult to twist in rapid kinetics and conversions of functional groups were lower than other samples (see Table 3). Unpolymerized carbon based chain segments in the system reduced the thermal stability.

3.3 Optical Properties

Due to the introduction of phenyl groups and sulfur atoms, TPS with high refractive indices exhibited favorable optical properties. Herein, the optical properties of UV-cured LPHs were further analyzed via UV-Vis spectrophotometer. Fig. 6 shows the transmittance of LPH films in the range of 300–800 nm wavelength. The spectrum indicated that LPH films had over 90% transmittance in the visible light range. In the range of 300–400 nm wavelength, the transmittance dropped rapidly due to the UV absorption of pendant phenyl groups which manifested UV shielding property. LPHs possessed low yellow indices as well, endowing excellent transparency. LPH01, LPH02 and LPH03 with high refractive index and light transmittance are

potentially suitable for UV shielding optical coatings and LPH04, LPH05 with medium refractive index are capable of combining with ultra high RI materials to fabricate high reflectance films like distributed Bragg reflectors [43].

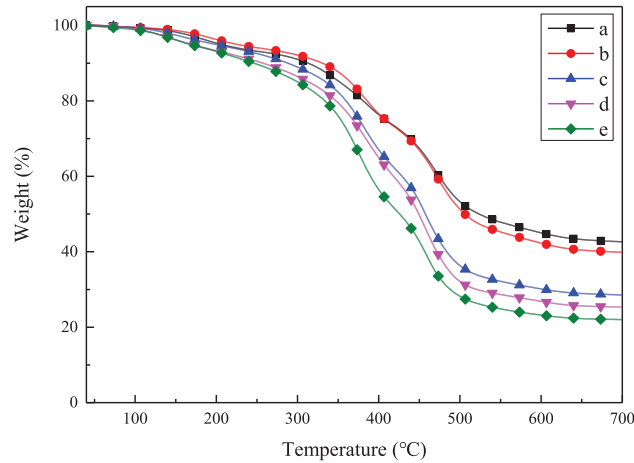


Figure 5: TGA curves of UV-cured LPHs. (a) LPH01, (b) LPH02, (c) LPH03, (d) LPH04 and (e) LPH05

Table 3: Thermal properties of UV-cured LPHs

Sample No.	$T_{5\%}$ (°C)	$T_{10\%}$ (°C)	R_w (%)
LPH01	205.99	313.33	42.64
LPH02	225.67	330.83	39.88
LPH03	198.67	288.50	28.56
LPH04	169.33	257.67	25.35
LPH05	167.67	246.50	22.03

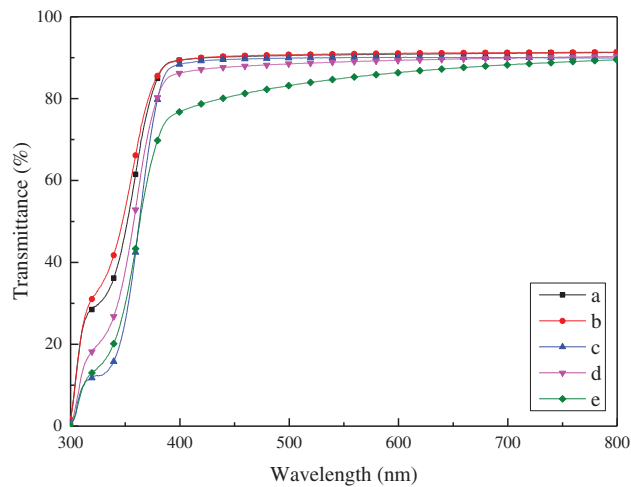


Figure 6: UV-Vis spectrum of LPH films with an average thickness of 200 μm (a) LPH01, (b) LPH02, (c) LPH03, (d) LPH04 and (e) LPH05. Note that the fluctuation of the signals appearing in the spectrum near 320 nm was caused by the instrument light converter

3.4 Moisture Barrier Properties

Optical and photovoltaic devices covered with barrier coatings could enhance moisture barrier properties and protect from corrosion. However, linalool contained a hydrophilic hydroxyl group that limited its utilizations in the application of functional barrier materials. We introduced rigid phenyl groups into flexible polysiloxane chains to reinforce moisture barrier properties and the water vapor permeability test results are shown in Table 4. As the phenyl content rose from 2.39 to 3.46 mmol/g, the water vapor permeability (WVP) value reduced to $1.10 \times 10^{-13} \text{ g}\cdot\text{cm}^{-1}\cdot\text{s}^{-1}\cdot\text{Pa}^{-1}$, demonstrating phenyl groups improved the moisture barrier properties of LPHs, which broadened the applications of linalool based hybrid materials in the field of optical barrier coatings.

Table 4: Optical properties, WVP values and WCA of LPH films

Sample No.	$T_{680\text{nm}}$	YI	WVP ($\times 10^{-13} \text{ g}\cdot\text{cm}^{-1}\cdot\text{s}^{-1}\cdot\text{Pa}^{-1}$)	Water contact angle ($^{\circ}$)
LPH01	91.04	0.013	1.10	91.10 ± 0.71
LPH02	91.21	0.013	1.29	92.33 ± 1.02
LPH03	90.03	0.009	2.13	96.30 ± 1.47
LPH04	89.80	0.029	2.48	95.16 ± 0.43
LPH05	87.95	0.108	2.77	88.42 ± 0.94

3.5 Water Contact Angle

To determine the moisture sensitivity of LPHs, the surface water contact angle was investigated and results were shown in Fig. 7. The WCA of LPH05 was 88.42° , which was attributed to a hydroxyl group in linalool structure weakening the hydrophobicity of UV-cured LPHs. While the phenyl content rose, the WCAs of LPH films were all over 90° , performing hydrophobicity. LPH03 and LPH04 had higher WCAs than other samples, which were caused by higher conversions of reactive functional groups and formed denser surfaces, exhibiting better moisture barrier properties.

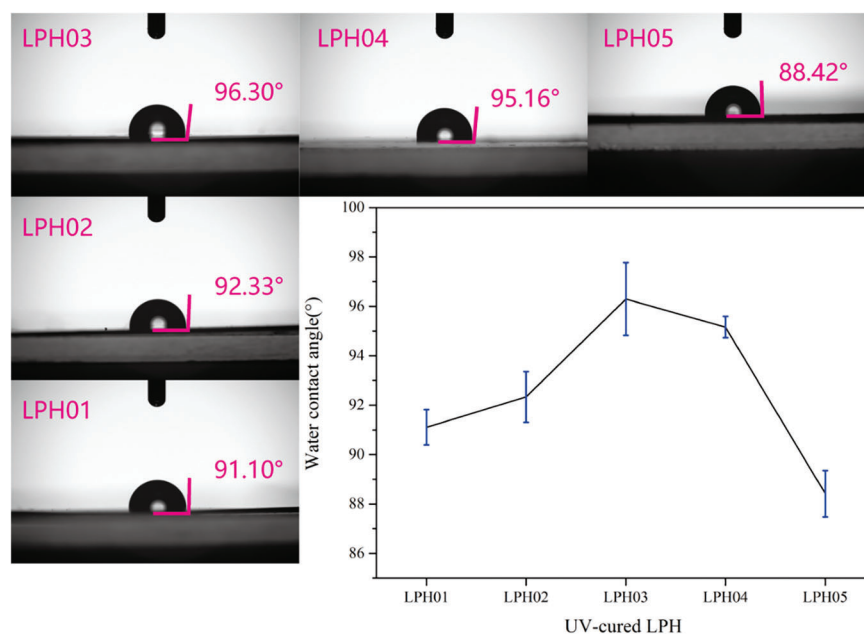


Figure 7: Water contact angles of UV-cured LPHs

3.6 UV Curing Behavior

As outlined in Fig. 8, LPHs were UV-cured at the intensity of 80 mW/cm^2 and the conversions of thiol groups and carbon-carbon double bonds were monitored by FT-IR. Fig. 8b shows the conversion of thiol group of LPH03 for 30 s UV irradiation. Absorption peak of thiol group at 2571 cm^{-1} decreased mostly for 5 s UV irradiation and disappeared completely for 10 s UV irradiation, demonstrating thiol group photocrosslinked rapidly in 5 s. Fig. 8c illustrates the conversion of double bonds of LPH03 for 30 s UV irradiation. The peak at 1638 cm^{-1} reduced substantially in 5 s UV irradiation and the peak intensity was maintained after 20 s UV irradiation. Though the double bond reacted in 20 s, slight peak signal was detected after 30 s irradiation. Polymer chains photocrosslinked in a high rate and the regular structure suffered steric hindrance, which resulted in the unsaturated double bond being difficult to twist and react sufficiently [44].

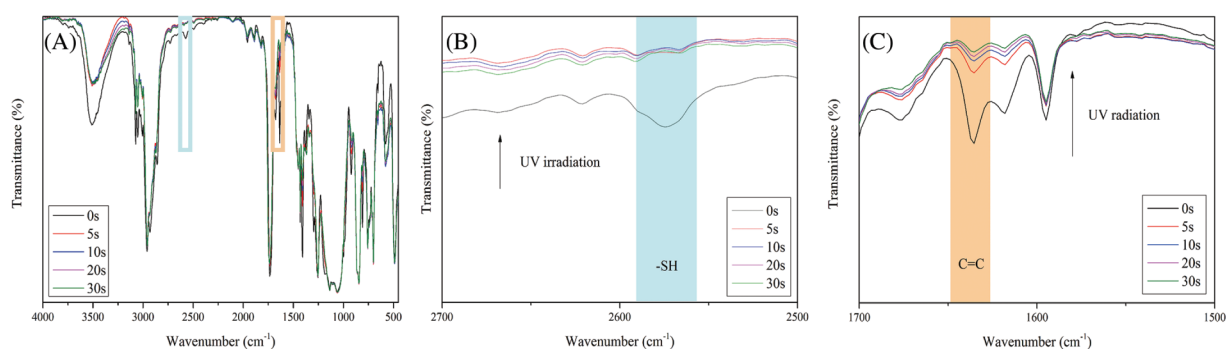


Figure 8: FTIR spectra of (A) LPH03 (B) thiol group (C) ene group for different UV irradiation times

All of the functional groups conversions of LPH films were analyzed by FT-IR and the results are demonstrated in Table 5. Apart from LPH01, thiol conversions of the rest LPHs were over 90%. Especially, thiol groups on LPH03, LPH04 and LPH05 with lower molecular weight reacted sufficiently which was unaffected by steric hindrance effect. At the same time, double bonds radical polymerized and had over 85% conversion. The conversion of ene groups in thiol-acrylate hybrid system has a close relationship with the molar ratio to thiol groups [45]. Due to the oxygen inhibition, ene groups have a low conversion generally. The introduction of thiol is capable to facilitate UV curing reaction efficiently and enhance the conversion of ene groups. However, when the thiol content is too high, it expeditiously reacts with double bonds and form a stable thioether structure which lowers the conversion of double bonds. Therefore, the ene group conversion shows a trend of first increasing and then decreasing as the thiol content increases.

Table 5: Thiol and ene groups conversions of LPHs for 30 s of UV irradiation

Sample No.	Thiol conversion (%)	Ene conversion (%)
LPH01	84.69	83.35
LPH02	90.22	85.05
LPH03	99.84	87.35
LPH04	99.02	93.97
LPH05	98.54	88.13

LPHs UV-cured under ambient conditions at the presence of PI-184. PI-184 cleaved and generated reactive free radicals after being irradiated by UV light. Reactive radicals triggered thiol group to generate thiyl radicals which were insensitive to oxygen. Thioether structure formed by the thiol addition across the ene groups and reactive radicals transferred to double bond and initiated further radical polymerizations [46]. LPHs photocrosslinked at a high reaction rate and unaffected by oxygen inhibition, performing excellent UV-curing properties.

The performances of related works are summarized in Table 6. Eugenol and soybean oil were utilized to manufacture bio-based coatings [47] and optical films [48] in some reported works. Compared with the related works, the bio-based hybrid films LPH were fabricated from a natural terpene linalool which was not previously reported. LPH films exhibited good optical properties and high curing efficiency.

Table 6: Performance comparison of this work and the related works

References	Bio-based source	Curing mechanism	Transmittance (%)	Refractive index	Curing efficiency
This work	Linalool	UV curing	91%	1.53	80 mW/cm ² UV irradiation for 20 s
[47]	Eugenol, soybean oil	UV curing	/	/	UV irradiation for 20 s
[48]	Eugenol	Thermal Curing	>90%	1.52	75°C for 10 h and 150°C for 3 h
[49]	/	UV curing	>80%	1.58	85 mW/cm ² UV irradiation for 3 min
[42]	/	UV curing	>90%	1.50	UV irradiation for 10 min

4 Conclusion

In this work, we synthesized thiol phenyl polysiloxanes (TPS) with various molecular weights via hydrolytic sol-gel reaction under acid conditions and fabricated UV-curing polysiloxane-linalool hybrid films (LPH) with natural terpene via thiol-ene reaction successfully. The designed structures of TPS were characterized by FT-IR, ¹H-NMR, ²⁹Si-NMR and GPC. The UV-cured LPHs exhibited high refractive indices and good optical transparency (over 90%). The introduction of phenyl groups enhanced the thermal stabilities and moisture barrier properties. LPHs could be rapidly prepared via photoinitiated thiol-ene reaction, showing a high reaction rate and high functional group conversions. It is believed that this research will broaden the utilization of linalool-polysiloxane hybrid materials in the fields of optical functional coatings.

Acknowledgement: The authors thank every author for their valuable suggestions, contribution and the fund for its support.

Funding Statement: The authors are grateful to the financial funding of the Guangdong Province Applied Science and Technology R&D Special Fund Project: Key Technologies for Industrialization of Sulfur-Resistant and High Refractive-Index LED Packaging Silicone Materials (2016B090930010).

Author Contributions: Formal analysis, Y. Ruan and L. Tan; Funding acquisition, X. Chen; Methodology, W. Xiao and Q. Li; Project administration, X. Chen; Writing—original draft, W. Xiao, and L. Tan; Writing—review & editing, W. Xiao, Q. Li and X. Chen. All authors have read and agreed to the published version of the manuscript.

Availability of Data and Materials: Data will be made available on request.

Conflicts of Interest: The authors declare that they have no conflicts of interest to report regarding the present study.

References

1. Chen, X., Yi, M., Wu, S., Tan, L., Xu, Y. et al. (2019). Synthesis of silphenylene-containing siloxane resins exhibiting strong hydrophobicity and high water vapor barriers. *Coatings*, *9*(8), 481.
2. Shang, X., Cao, X., Ma, Y., Kumaravel, J. J., Zheng, K. et al. (2018). Diphenylsiloxane-bridged ladder-like hydrido-polysiloxane and the derivatisation by triphenylsiloxy substitution. *European Polymer Journal*, *106*, 53–62.
3. Zhang, Y., Xu, Y., Simon-Masseron, A., Lalevée, J. (2021). Radical photoinitiation with LEDs and applications in the 3D printing of composites. *Chemical Society Reviews*, *50*(6), 3824–3841.
4. Pan, Z., Cheng, Y., Zhang, Z. (2022). Synthesis of high refractive index silicone LED encapsulation with ultra-high hardness. *Silicon*, *14*(12), 1–8.
5. Shen, J., Feng, Y. (2023). Recent advances in encapsulation materials for light emitting diodes: A review. *Silicon*, *15*(5), 2163–2172.
6. Chen, X., Fang, L., Wang, J., He, F., Chen, X. et al. (2018). Intrinsic high refractive index siloxane-sulfide polymer networks having high thermostability and transmittance via thiol-ene cross-linking reaction. *Macromolecules*, *51*(19), 7567–7573.
7. Tasdelen, M. A., Lalevée, J., Yagci, Y. (2020). Photoinduced free radical promoted cationic polymerization 40 years after its discovery. *Polymer Chemistry*, *11*, 1111–1121.
8. Liu, F., Liu, A., Tao, W., Yang, Y. (2020). Preparation of UV curable organic/inorganic hybrid coatings—a review. *Progress in Organic Coatings*, *145*, 105685.
9. Bakhshandeh, E., Sobhani, S., Croutxé-Barghorn, C., Allonas, X., Bastani, S. (2021). Siloxane-modified waterborne UV-curable polyurethane acrylate coatings: Chemorheology and viscoelastic analyses. *Progress in Organic Coatings*, *158*, 106323.
10. Jeong, K. M., Park, S. S., Nagappan, S., Jin, H., Min, G. et al. (2021). Transparent and hard siloxane based hybrid UV-curable coating materials with amphiphobic properties. *Journal of Nanoscience and Nanotechnology*, *21*(8), 4450–4456.
11. Atici, Y., Emik, S., Kırbaslar, Ş.İ. (2022). Effect of siloxane chain length on thermal, mechanical, and chemical characteristics of UV (ultraviolet)-curable epoxy acrylate coatings. *Journal of Coatings Technology and Research*, *19*(2), 439–451.
12. O'Bryan, C. S., Bhattacharjee, T., Hart, S., Kabb, C. P., Schulze, K. D. et al. (2017). Self-assembled micro-organogels for 3D printing silicone structures. *Science Advances*, *3*(5), e1602800.
13. Foerster, A., Annarasa, V., Terry, A., Wildman, R., Hague, R. et al. (2021). UV-curable silicone materials with tuneable mechanical properties for 3D printing. *Materials & Design*, *205*, 109681.
14. Ning, L., Chen, J., Sun, J., Liu, Y., Yi, D. et al. (2021). Preparation and properties of 3D printing light-curable resin modified with hyperbranched polysiloxane. *ACS Omega*, *6*(37), 23683–23690.
15. Ford, M. J., Loeb, C. K., Pérez, L. X. P., Gammon, S., Guzorek, S. et al. (2022). 3D Printing of transparent silicone elastomers. *Advanced Materials Technologies*, *7*(5), 2100974.
16. Gan, Y., Jiang, X., Yin, J. (2014). Thiol-ene photo-curable hybrid silicone resin for LED encapsulation: Enhancement of light extraction efficiency by facile self-keeping hemisphere coating. *Journal of Materials Chemistry C*, *2*(28), 5533–5539.
17. Kermainejad, H., Najafi, F., Soleimani-Gorgani, A. (2019). Encapsulation of flexible organic light emitting diodes by UV-cure epoxy siloxane. *Journal of Applied Polymer Science*, *136*(41), 48033.
18. Shi, X., Zhang, K., Chen, J., Qian, H., Huang, Y. et al. (2023). Octopi tentacles-inspired architecture enables self-healing conductive rapid-photo-responsive materials for soft multifunctional actuators. *Advanced Functional Materials*, 2311567.

19. Liu, Z., Hong, P., Huang, Z., Zhang, T., Xu, R. et al. (2020). Self-healing, reprocessing and 3D printing of transparent and hydrolysis-resistant silicone elastomers. *Chemical Engineering Journal*, 387, 124142.
20. Shang, X., Duan, S., Zhang, M., Cao, X. Y., Zheng, K. et al. (2018). UV-curable ladder-like diphenylsiloxane-bridged methacryl-phenyl-siloxane for high power LED encapsulation. *RSC Advance*, 8(17), 9049–9056.
21. Jung, K. I., Hwang, S. O., Kim, N. H., Lee, D. G., Lee, J. H. et al. (2018). Effect of methacryloxypropyl and phenyl functional groups on crosslinking and rheological and mechanical properties of ladder-like polysilsesquioxane hard coatings. *Progress in Organic Coatings*, 124, 129–136.
22. Ye, H., Zhang, X. S., Li, Y. J., Wang, T. (2012). Synthesis and cationic photopolymerization of phenyl epoxy-silicone monomers. *Journal of Polymer Research*, 19(12), 1–6.
23. Yang, S., Kwak, S., Jin, J., Kim, J. S., Choi, Y. et al. (2012). Thermally resistant UV-curable epoxy-siloxane hybrid materials for light emitting diode (LED) encapsulation. *Journal of Materials Chemistry*, 22(18), 8874–8880.
24. Jiang, B., Shi, X., Zhang, T., Huang, Y. (2022). Recent advances in UV/thermal curing silicone polymers. *Chemical Engineering Journal*, 435, 134843.
25. Mondal, T. (2021). Radiation curable polysiloxane: Synthesis to applications. *Soft Matter*, 17(26), 6284–6297.
26. Li, X., Bian, F., Hu, J., Li, S., Gui, X. et al. (2022). One-step synthesis of novel multifunctional silicone acrylate prepolymers for use in UV-curable coatings. *Progress in Organic Coatings*, 163, 106601.
27. Bian, F., Li, X., Zhao, J., Hu, J., Gui, X. et al. (2023). One-step synthesis of epoxy-based silicon prepolymers and its application in UV-curable coating. *Journal of Coatings Technology and Research*, 20(1), 321–331.
28. O'Brien, A. K., Cramer, N. B., Bowman, C. N. (2006). Oxygen inhibition in thiol-acrylate photopolymerizations. *Journal of Polymer Science, Part A: Polymer Chemistry*, 44(6), 2007–2014.
29. Oytun, F., Kahveci, M. U., Yagci, Y. (2013). Sugar overcomes oxygen inhibition in photoinitiated free radical polymerization. *Journal of Polymer Science, Part A: Polymer Chemistry*, 51(8), 1685–1689.
30. Ping, T., Zhou, Y., He, Y., Tang, Y., Yang, J. et al. (2016). Preparation and characterization of yellowing resistance and low volume shrinkage of fluorinated polysiloxane urethane acrylate. *Progress in Organic Coatings*, 97, 74–81.
31. Resetco, C., Hendriks, B., Badi, N., Du Prez, F. (2017). Thiol-ene chemistry for polymer coatings and surface modification-building in sustainability and performance. *Materials Horizons*, 4(6), 1041–1053.
32. Zhang, W., Wang, R., Yang, Z., Bai, Y., Meng, L. et al. (2023). Synthesis of UV rapid curing silicone coatings via photoinitiated thiol-ene click polymerization for pressure-sensitive adhesive. *Polymer*, 283, 126222.
33. Bhagat, S. D., Chatterjee, J., Chen, B., Stiegman, A. E. (2012). High refractive index polymers based on thiol-ene cross-linking using polarizable inorganic/organic monomers. *Macromolecules*, 45(3), 1174–1181.
34. Kim, J. S., Yang, S., Park, H., Bae, B. S. (2011). Photo-curable siloxane hybrid material fabricated by a thiol-ene reaction of sol-gel synthesized oligosiloxanes. *Chemical Communications*, 47(21), 6051–6053.
35. Noè, C., Iannucci, L., Malburet, S., Graillot, A., Sangermano, M. et al. (2021). New UV-curable anticorrosion coatings from vegetable oils. *Macromolecular Materials and Engineering*, 306(6), 2100029.
36. Zheng, J., Cai, Y., Zhang, X., Wan, J., Fan, H. (2022). Eugenol-based siloxane acrylates for ultraviolet-curable coatings and 3D printing. *ACS Applied Polymer Materials*, 4(2), 929–938.
37. Herman, A., Tambor, K., Herman, A. (2016). Linalool affects the antimicrobial efficacy of essential oils. *Current Microbiology*, 72(2), 165–172.
38. Modjinou, T., Versace, D. L., Abbad-Andallousi, S., Bousserhine, N., Dubot, P. et al. (2016). Antibacterial and antioxidant bio-based networks derived from eugenol using photo-activated thiol-ene reaction. *Reactive and Functional Polymers*, 101, 47–53.
39. Yi, M., Chen, X., Wu, S., Ge, J., Zhou, X. et al. (2018). Fabrication of reactive poly(phenyl-substituted siloxanes/silsesquioxanes) with Si-H and alkoxy functional groups via the Piers-Rubinsztajn reaction. *Polymers*, 10(9), 1006.
40. Lee, A. S., Jo, Y. Y., Jeon, H., Choi, S. S., Baek, K. Y. et al. (2015). Mechanical properties of thiol-ene UV-curable thermoplastic polysilsesquioxanes. *Polymer*, 68, 140–146.

41. Cole, M. A., Bowman, C. N. (2012). Synthesis and characterization of thiol-ene functionalized siloxanes and evaluation of their crosslinked network properties. *Journal of Polymer Science, Part A: Polymer Chemistry*, 50(20), 4325–4333.
42. Macdonald, E. K., Shaver, M. P. (2015). Intrinsic high refractive index polymers. *Polymer International*, 64(1), 6–14.
43. Kleine, T. S., Diaz, L. R., Konopka, K. M., Anderson, L. E., Pavlopoulos, N. G. et al. (2018). One dimensional photonic crystals using ultrahigh refractive index chalcogenide hybrid inorganic/organic polymers. *ACS Macro Letters*, 7(7), 875–880.
44. Kim, Y. H., Choi, G. M., Bae, J. G., Kim, Y. H., Bae, B. S. (2018). High-performance and simply-synthesized ladder-like structured methacrylate siloxane hybrid material for flexible hard coating. *Polymers*, 10(4), 449.
45. Zhang, J., Li, L., Guo, R., Zhou, H., Li, Z. et al. (2019). Preparation of novel UV-cured methacrylate hybrid materials with high thermal stability via thiol-ene photopolymerization. *Journal of Materials Science*, 54(7), 5877–5897.
46. Sahin, M., Ayalur-Karunakaran, S., Manhart, J., Wolfahrt, M., Kern, W. et al. (2017). Thiol-ene versus binary thiol-acrylate chemistry: Material properties and network characteristics of photopolymers. *Advanced Engineering Materials*, 19(4), 1–10.
47. Zhang, D., Liang, H., Bu, J., Xiong, L., Huang, S. et al. (2015). UV curable soybean-oil hybrid systems based on thiol-acrylate and thiol-ene-acrylate chemistry. *Journal of Applied Polymer Science*, 132(24), 42095.
48. Yi, M., Chen, X., Shuttleworth, P. S., Tan, L., Ruan, Y. et al. (2021). Facile fabrication of eugenol-containing polysiloxane films with good optical properties and excellent thermal stability via Si-H chemistry. *Journal of Materials Chemistry C*, 9(25), 8020–8028.
49. Hoyle, C. E., Lee, T. Y., Roper, T. (2004). Thiol-enes: Chemistry of the past with promise for the future. *Journal of Polymer Science, Part A: Polymer Chemistry*, 42(21), 5301–5338.